Journal of Applied Biomaterials & Biomechanics 2004; 2: 112-119

Bone response to zinalco implants

C. PIÑA[1], E. VILLARREAL[1], S. MARTÍN[2], B. LEÓN[2], G. TORRES-VILLASEÑOR[1], P. BOSCH[1]

[1]Institute of Investigations on Materials, UNAM
[2]Faculty of Medicine, UNAM, University Town, Mexico City - Mexico

ABSTRACT: *The evolution of dog femur bone implanted* in vivo *with either steel or with a metal alloy (zinalco), was compared at different time-periods ≤9 months. Bone behavior was studied by radiology, scanning electron microscopy (SEM), thermogravimetric analysis (TGA) and Fourier transform infrared spectroscopy (FTIR) and it was shown that zinalco corroded whereas the steel remained unaltered in the presence of body fluids. Small amounts of metal ions were released continuously, promoting disordered bone growth enriched with organic tissue. After 9 months, the organism managed to compensate for this effect and the proportion of mineral to organic tissue resulted in being normal, although it was unable to correct the shape and the direction of the growth. (Journal of Applied Biomaterials & Biomechanics 2004; 2: 112-9)*

KEY WORDS: *Zinalco, Steel, Bone implants, SEM, TGA, FTIR,* In vivo *test, Zinc, Citotoxicity*

Received 23/05/03; Revised 01/09/03; Accepted 17/10/03

INTRODUCTION

When a metallic alloy encounters physiological fluids it corrodes releasing small metal particles and ions that are accommodated in the surrounding tissues or are incorporated in the blood. The released metal ions can follow the same metabolic routes as the essential life ions. They can then participate in unsuitable oxidation reactions and/or interfere in ion exchange processes (1). Some metallic ions play an important role in bone regeneration, as the enzyme associated with osseous growth requires these ions. In fact, bone cell differentiation and proliferation require enzymes whose activity depends on metals like copper (Cu) and zinc (Zn) (2).

The most commonly used metallic implants are titanium, titanium alloys and special stainless steel. Nevertheless, new materials are being tested continuously to improve prostheses performance. In this context, zinalco alloy should be tested as a promising material, with adequate mechanical properties to substitute bone; its composition is 80% Zn, 18% aluminum (Al) and 2% Cu (3). Furthermore, in previous studies, we demonstrated through SMART testing that in wing cells of the fruit fly *Drosophila melanogaster* zinalco was not genotoxic (4). The effect of zinalco on the mitotic index was studied to detect cell damage in cultured human lymphocytes; there were no differences between controls and samples exposed to 5, 50 or 200 µg/ml (5-7). Therefore, zinalco was not cytotoxic with lymphocytes, as there were no observed clastogenic or aneugenic effects.

Following the standard biocompatibility tests indicated by ASTM, zinalco alloy, shaped as small plaques, was implanted subcutaneously and intramuscularly in rats. After 8 months, there was no evidence of Zn, Al, or Cu presence in the blood. There was neither toxicity nor rejection. Furthermore, the implanted rats resulted in being healthier than the control rats implanted with 316L-SS steel (8-10).

When four dogs were implanted with zinalco and 316L-SS cylinders at proximal distal thirds to the right femur, bone formation adjacent to the implants occurred. There were no severe periosteal irregular reactions nor osseous reabsorption or rejection. The Zn, Al or Cu concentrations in the

1722-6899/112-08$15.00/0

blood of the implanted dogs did not change (11). This aimed to test zinalco as a biomaterial for use as an orthopedic implant. Therefore, mongrel dogs were implanted with intramedullar zinalco nails. For comparison, 316L-SS nails were used because 316L-SS is a well-known biomaterial. The bone modifications were studied by radiography, by scanning electron microscopy (SEM), by thermogravimetric analysis (TGA) and by Fourier transform infrared spectroscopy (FTIR) after 1, 2, 3, 6 and 9 months.

MATERIALS AND METHODS

Nails: The zinalco nails were extruded and the 316L-SS nails were commercial. After ultrasonic cleaning and sterilization in an autoclave, the zinalco and the commercial 316L-SS nails (cylindrically shaped, 4 mm x 10 cm) were inserted under aseptic conditions.

Animals: Fifteen male 2-year-old mongrel dogs in good health, whose body weight range was 8-10 kg, were implanted in the right femur, 10 of them intramedullar with a zinalco nail and the other five with 316L-SS. The experimentation periods were 1, 2, 3, 6, and 9 months. In each period two dogs implanted with zinalco and one dog implanted with 316L-SS were humanely killed; therefore, the zinalco effect was observed in two dogs, but in only one dog for the 316L-SS effect as a control. The dogs were pre-anesthetized with xylacine 1 mg/kg/i.m., and then anesthetized with pentobarbital 25 mg/kg/i.v. and atropine 0.01 mg/kg/i.v. as an anticholinergic. General inhaled anesthesia was not used as the surgical procedure, because the time was <30 min (12-15). These are the biomedical research principles involving animals that are studied at the Universidad Nacional Autónoma de México (16).

Surgery: A longitudinal incision of approximately 5 cm was made on the outside part of the thigh the periosteum was then opened and cut. The femur in the diafisis zone was broken using pincers. The intramedullar nail was implanted and the surgery controlled by radiography. The nail was cut at bone level. After surgery, the implanted leg was immobilized with gypsum for 15 days and dicloxacilin (55 mg/kg/8hr/PO) was administered for 5 days to avoid wound infections.

The animals were housed under a constant temperature (20 ± 2 °C), relative humidity (50 ± 10%) and light-dark periodicity (L:D 12:12). During the experiment, water and food were supplied *ad libitum*. Each month, radiography was performed to evaluate the fracture repair process, as well as the nail-bone interaction degree.

Specimen processing: Two dogs implanted with zinalco and one dog with 316L-SS were humanely killed at each experimental period and the implanted femur bone extracted. The implanted bones were fixed in 10% buffer formaldehyde for 7 days, cut width ways to obtain cylindrical samples of 2-3 mm in length, and finally embedded in an epoxy resin. The samples obtained were characterized by SEM, TGA, differential thermal analysis (DTA) and FTIR. A Philips Diagnost 70 was employed for the radiographical studies. A Leica-Cambridge Stereoscan 440 microscope was used for SEM. The samples were dehydrated for 2 days and sputter-coated in gold. For TGA and DTA, the tissue was previously fixed, dried and pulverized in an agate mill, a thermal analysis system (9900, Du Pont 951) was utilized. The samples (5-10 mg) were heated in a platinum crucible in air at 10 °C/min to 1000 °C. The FTIR spectra were obtained in a Nicolet 680 in the range 4100-300 cm^{-1}. The powdered samples, mixed with KBr (1:100), were compacted to form a pellet.

RESULTS

Clinic: There were no rejections, no infections and no disease symptoms in the implanted dogs. Furthermore, the wounds healed in normal time for all dogs. However, only dogs implanted with 316L-SS could support their right hind leg. Although this observation could have indicated malpositioning of the intramedullary nails, a fracture non-union or a pseudoarthrosis, the good recovery of the 316L-SS implanted dogs demonstrated that this was not the case. Furthermore, 316L-SS and zinalco nails were identical in shape and were implanted using the same method and in the same position.

Radiological study: There was a monthly radiograph of each dog to follow the injured tissue recovery process, the implant position and the tissue reaction to the implant. Figure 1a shows a radiograph of the pelvic hip with the right femur implanted with 316L-SS immediately post-surgery. In Figure 1b, the regeneration process is already evident, only 1 month has passed since surgery. Figure 1c shows a fully recovered bone corresponding to 2 months post-surgery.

Figure 2a shows a radiograph of the zinalco implants immediately post-surgery, it was very similar for all implantations. In Figures 2b and 2c the femur bone appears less dense as the volume increases with time.

SEM: The interface and the morphology of the bone samples were studied by SEM, because with

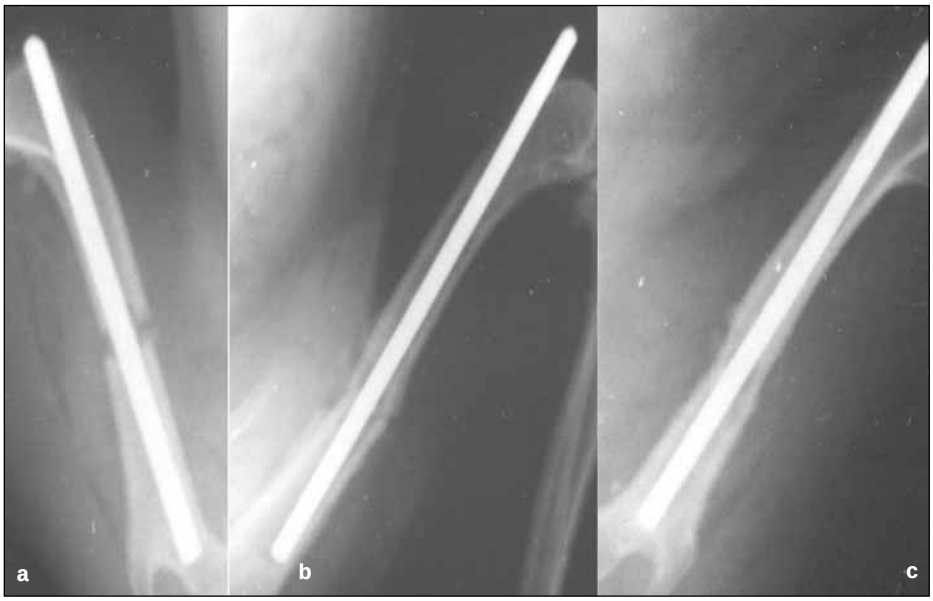

Fig. 1 - *a) Radiograph of the pelvic hip with the right femur implanted with 316L-SS immediately postsurgery. The fracture of femur is clearly visible. b) Radiograph of the pelvic hip with the right femur implanted with 316L-SS, 1 month post-surgery. c) Radiograph of the pelvic hip with the right femur implanted with 316L-SS, 2 months post-surgery. A fixation can be seen or bony regeneration in the fracture zone, bony callus is not observed because the process is complete.*

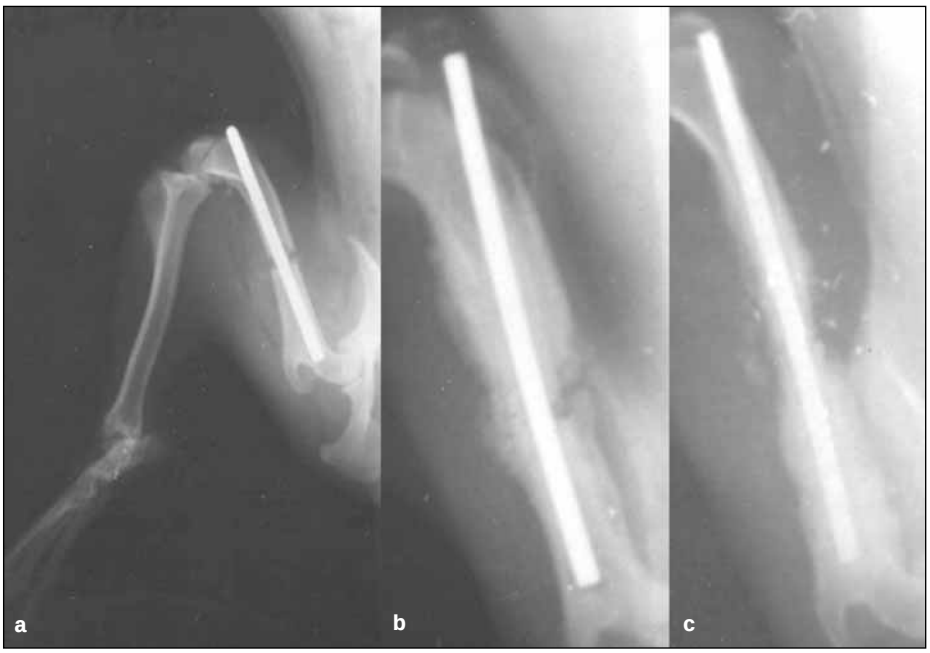

Fig. 2 - *a) Radiograph of the pelvic hip with the right femur implanted with zinalco immediately post-surgery. b) Radiograph of the pelvic hip with the right femur implanted with zinalco, 1 month post-surgery. c) Radiograph of the pelvic hip with the right femur implanted with zinalco, 2 months post-surgery. A periostic reaction is visible; the bone regeneration is not normal.*

SEM the samples did not have to be decalcified. The 316L-SS implants were healthy and with compacted bone around the implant, particularly in the surgery zone. Figure 3a shows the implant and the bone 3 months post-surgery. Figure 3b shows the transversal zone, immediate to the implant 9 months post-surgery. The steel implant was removed easily because the bone had not adhered to it.

Three months post-surgery the bone had adhered to the zinalco implant (Fig. 4a); however, after 9 months the bone morphology had definitely altered (Fig. 4b); bone structure was lost, and the bone was not compact and resulted in being porous. Figure 4c shows the tissue disorganization.

DTA-TGA: Figure 5 shows the TGA curves of healthy bone. Initially, from room temperature to 200 °C, water was lost, then from 200 to 450 °C, organic matter had decomposed and finally, from 450 to 650 °C, organic residues were burnt; >650 °C, the inorganic phase only of the bone remained (17-19).

Figure 6 compares the 316L-SS- and zinalco-implanted bone thermograms. The 316L-SS thermograms reproduced the previous curve and showed that the residual inorganic phase was approximately 58 wt% after 1 month and 61% after 3

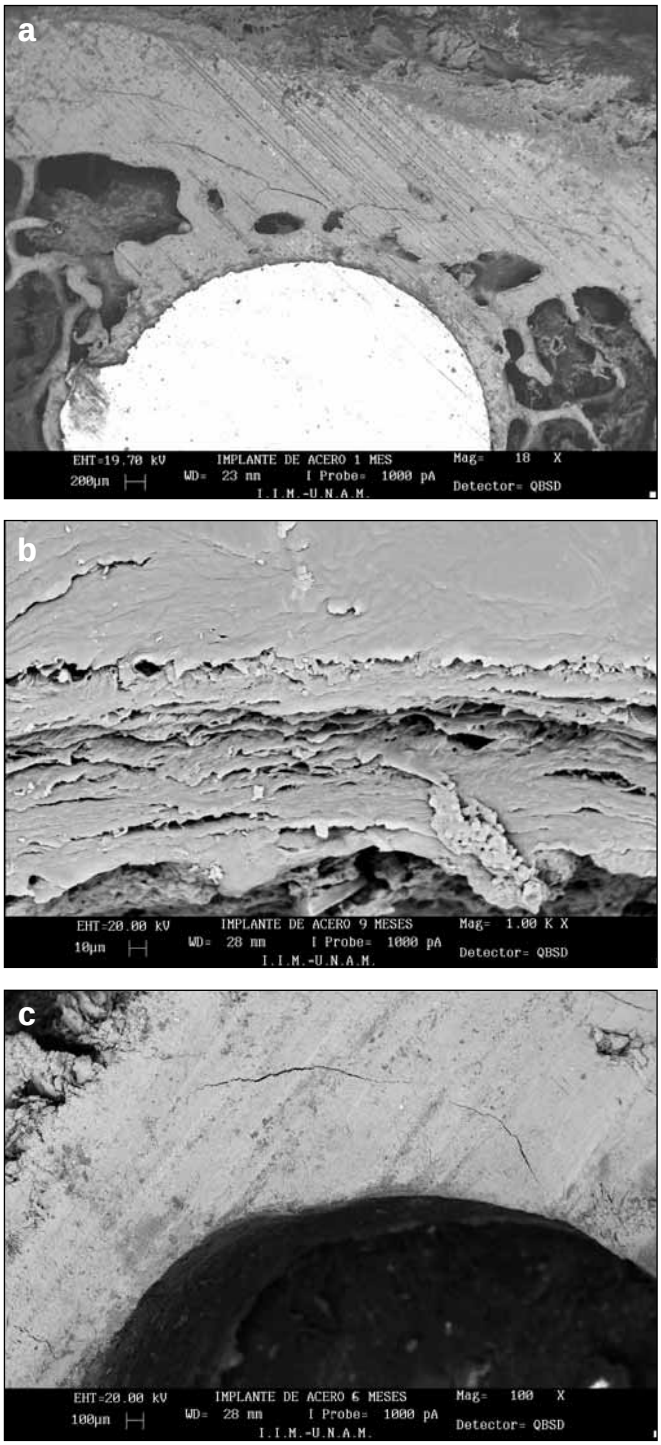

Fig. 3 - *a) Microstructure of bone surrounding 316L-SS implant 1 month post- surgery. b) Microstructure of bone surrounding 316L-SS implant 9 months post-surgery. c) Microstructure of bone surrounding 316L-SS implant 6 months post-surgery.*

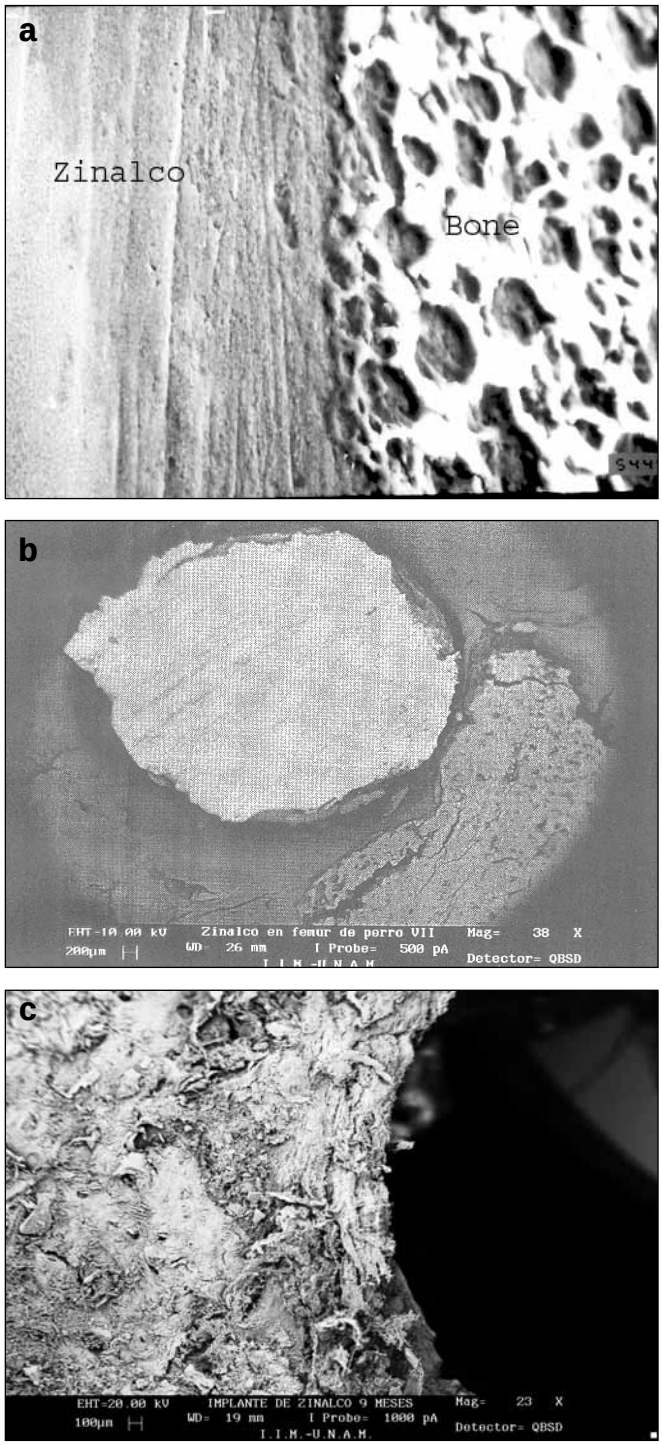

Fig. 4 - *a) Microstructure of bone surrounding zinalco implant 1 month post-surgery. b) Microstructure of bone surrounding zinalco implant 3 months post-surgery. c) Microstructure of bone surrounding zinalco implant 9 months post-surgery.*

months. The thermograms corresponding to zinalco implanted bones showed that after 1 month, the proportion of the organic phase was unusually high as the residual inorganic phase was only 20%. This percentage increased to 55% for inorganic compounds after 9 months, this value was similar to the amount present in the healthy bone. Furthermore, note that the DTA curves were the same in all samples and similar to the healthy bone curve.

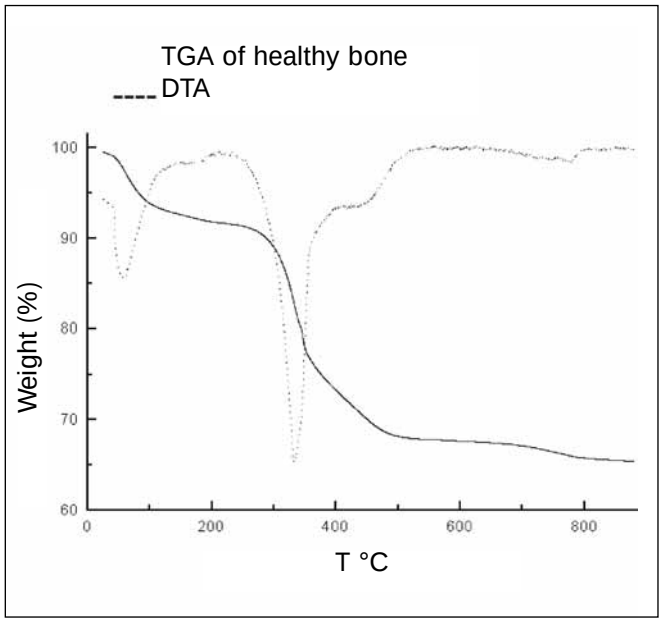

Fig. 5 - *TGA obtained for healthy bone (14).*

This variation of mineral to organic tissue is clear in Figure 7, where the percentage of mineral phase was plotted as a function of time.

FTIR: Figures 8 and 9 compare the infrared spectra after 1, 3, 6 and 9 months for the 316L-SS and the zinalco implanted bones, respectively. All FTIR bands can be interpreted conventionally as shown in Table I (20-23), they were present in all patterns. In comparing the 316L-SS implanted bone spectra, the main difference was the intensity of the band at 1098-1050 cm^{-1}, which corresponded to a P-O stretch vibration. This band is a feature of young bone and it reached its maximum in the 6-month sample; in the 9-month sample, the most intense band was at 1700-1595 cm^{-1}, which corresponded to amide I. Instead, in zinalco implanted bone, although the bands were the same, the P-O stretching was always very intense. After 6 months, the spectra of 316L-SS and Zinalco implanted samples were very similar, showing a close-knit composition.

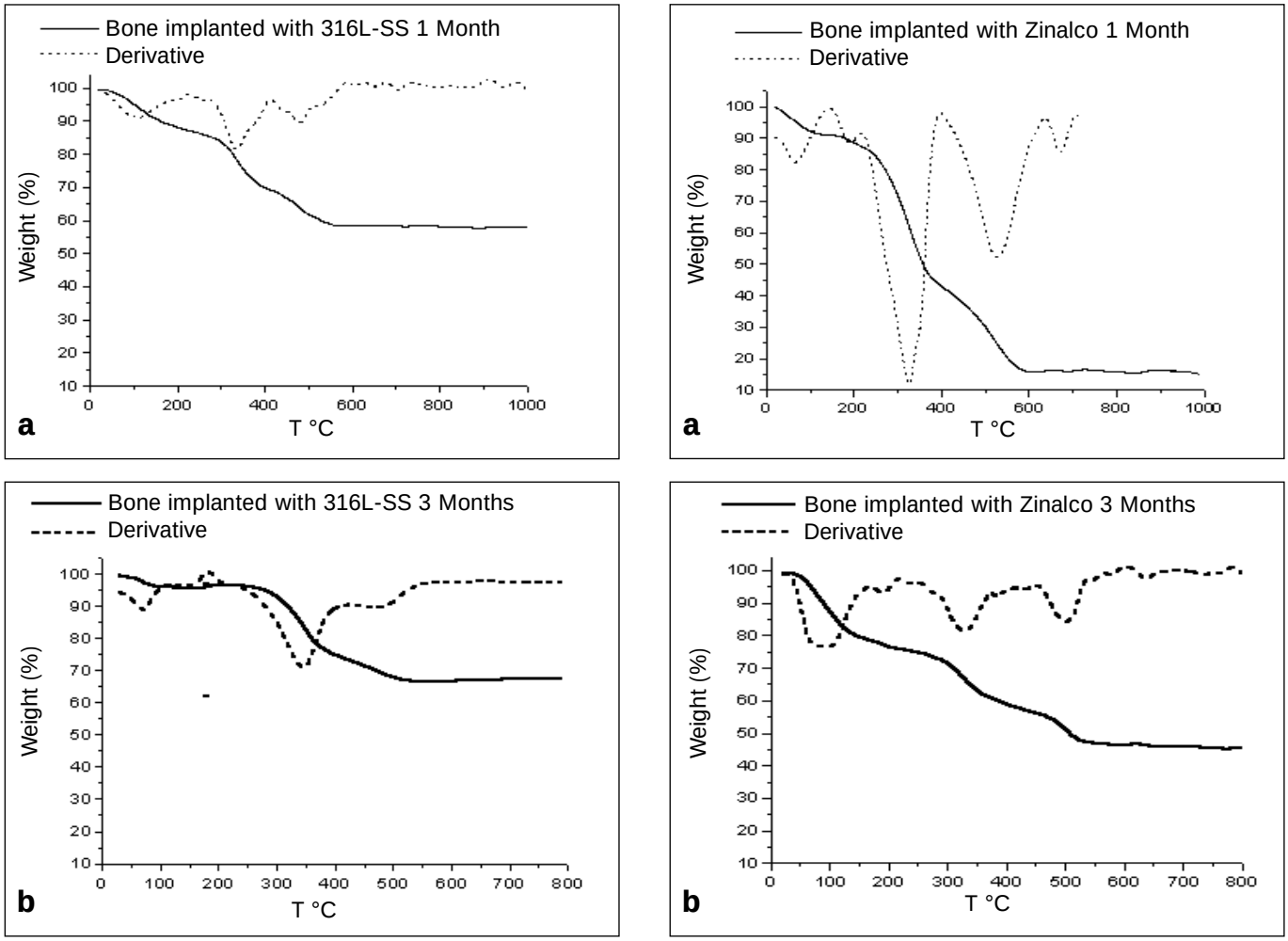

Fig. 6 a, b - *Comparison of TGA obtained for bones implanted with 316L-SS and zinalco after 1 and 3 months.*

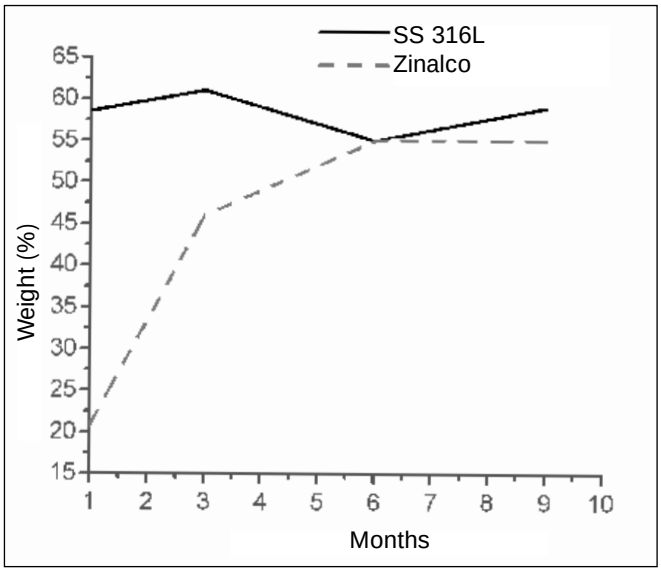

Fig. 7 - *Comparison of mineral wt% for 316L-SS and zinalco implanted bones as a function of time.*

TABLE I - ASSIGNMENT OF THE FTIR BANDS

Band position (cm^{-1})	Assignment
3450-3300	OH stretching
3100-2900	Lipids and carbonates
1740	C=O
1700-1595	Amide I
1565-1550	Amide II
1500-1400	Carbonates
1250	P-OH deformation
1098-1050	P-O stretching
988-960	P-O stretching
890-840	Carbonates
610-525	Phosphates (PO_4^{-3} scissors vibration)
470	O-P-O scissors vibration

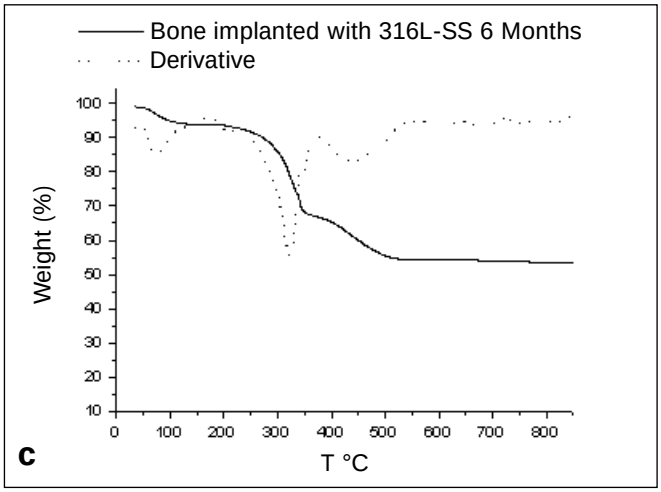

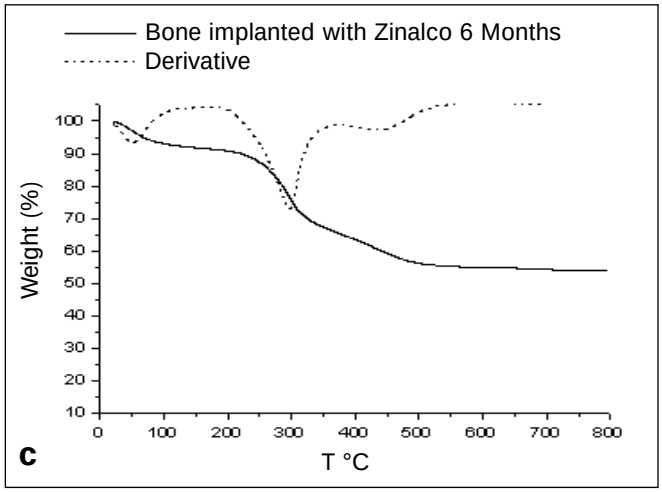

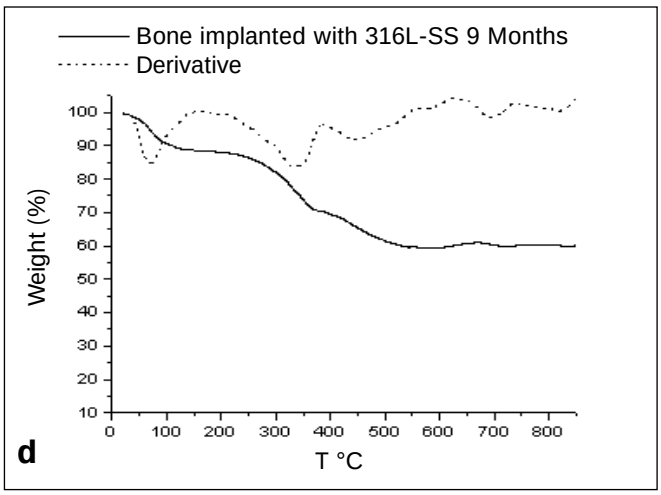

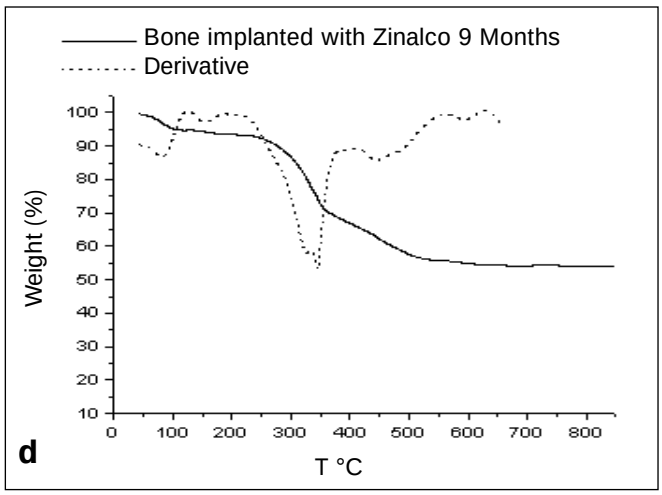

Fig. 6 c, d - *Comparison of TGA obtained for bones implanted with 316L-SS and zinalco after 6 and 9 months.*

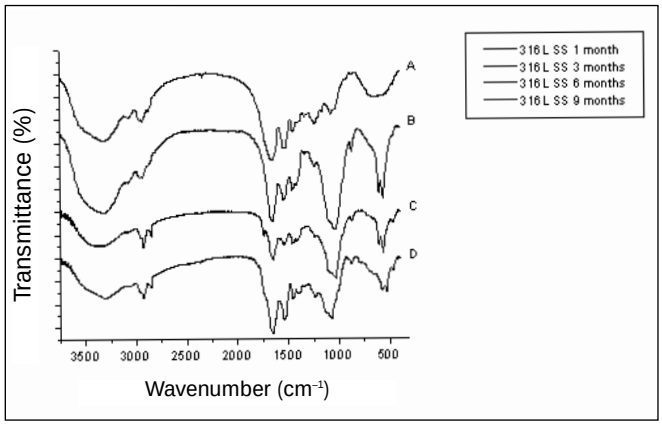

Fig. 8 - *Infrared spectra after 1, 3, 6 and 9 months for 316L-SS implanted bones.*

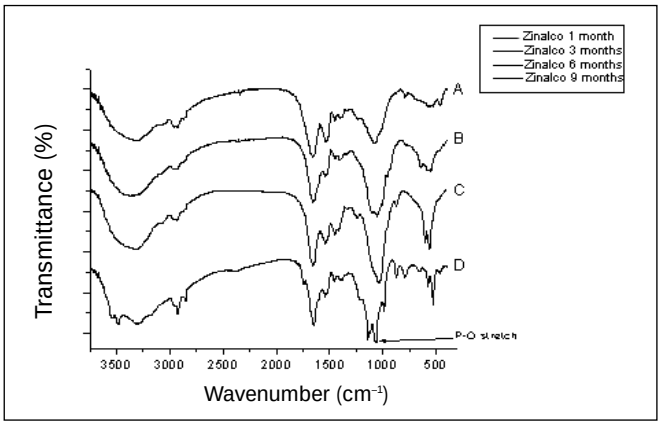

Fig. 9 - *Infrared spectra after 1, 3, 6 and 9 months for zinalco implanted bones.*

DISCUSSION

Several characterization techniques were used to compare the evolution over time of 316L-SS and Zinalco implanted bones. The results seemed to contradict our previous studies *in vivo* and *in vitro*, where zinalco appeared to be rather innocuous if in contact with vivid matter. Indeed, zinalco implanted bone behaved in a very different way than the 316L-SS implanted bone. From a macroscopic approach, zinalco implanted bone grew loosing its apparent density and strength.

In this sense, microscopy images were the most illustrative as the zinalco and bone interface were corroded. Therefore, small particles and ions of the metals present in the alloy were free to react with bone tissue. It has been often reported that Zn, which is the main component of the alloy, can, if in small amounts (traces), promote bone formation but, in high concentration, it causes cytotoxicity (24). Zn inhibits osteoclastic bone resorption *in vitro*. However, it has to be emphasized that as long as Zn bonds to the metal alloy, it is "safe", but when ions and small metal particles are incorporated in the tissue, the bone responds with the effects reported in this study. The Zn effect could explain, in this way, the irregular bone growth found in the 1st month in the zinalco implanted bone.

The FTIR results agreed with the above results, as initially (1 month) the P-O vibration was very intense in zinalco implanted bone; this was not the case in 316L-SS implanted bone. This vibration, which was the main difference between the two groups of samples, was characteristic of young bone and poorly crystalline hydroxyapatite. Therefore, it seems that due to Zn presence the hydroxyapatite was unorganized and less stable. After 6 months, when the mineral to organic ratio was the same in both implanted bone samples, the zinalco implanted bone remained disordered, and a callous phosphorous enriched tissue formed, which was stable to 500 °C, as shown in DTA-TGA analyzes.

TGA results indicated that initially the proportion of the mineral phase was, in steel, twice the amount found in zinalco implanted bone. Over time, the composition of both implanted bone samples resulted in being similar corresponding to healthy bone, but zinalco implanted bone was already shapeless. Therefore, the normal growth and mineralization mechanisms as those observed in the 316L-SS implanted bones were altered by the interaction with the metal alloy.

CONCLUSIONS

The comparative study of 316L-SS and zinalco implanted bones after 1 month demonstrated that Zn was released in the surrounding tissue of the implant by the corroded zinalco alloy. After 6 months, the ratio of mineral to organic tissue was the same for both implants, although bone growth in the zinalco implanted dogs was disordered and the dogs could not use their right hind leg: hydroxyapatite is poorly crystalline. Zinalco not only released a high amount of Zn, which can be toxic, but it released it as ions and small particles, which locally promoted inflammation. The growth mechanism of the corresponding bone altered. Most interesting was the organism response, which managed to resorb this organic tissue and after 6 months reach the normal proportion of mineral to organic tissue. However, it was unable to correct the shape and the direction of the growth.

ACKNOWLEDGEMENTS

The authors wish to thank DGAPA-UNAM and CONACYT for financial support, and José Ocotlán Flores, Carlos Flores, Carmen Vázquez and Raúl Reyes, for their technical support.

Address for correspondence:
Dr. Cristina Pina
Instituto de Investigaciones en Materiales
UNAM A.P. 70-360
México 04510
D.F. - Mexico
mcpb@servidor.unam.mx

REFERENCES

1. Silver FH, Christiansen DL. In: Biomaterials Science and Biocompatibility. New York: Springer-Verlag 1999; 1-3.
2. Yamaguchi M, Kishi S. Zinc compounds inhibit osteoclast-like cell formation at the earlier stage of rat marrow culture but not osteoclast function. Mol Cell Biochem 1996; 158: 171-7.
3. Torres Villaseñor G. Microestructura y propiedades mecánicas del Zinalco. Ciencias 1988; 39: 103-11.
4. Guzmán Rincón J, Ramírez Victoria P, Martínez Ocampo A, Piña Barba C. Genotoxicity valuation of the zinalco (TM) in drosophila melanogaster. In: Torres G, Piña C, Zhu Y, eds. Advances in Science, Technology and Applications of Zn-Al Alloys, 3rd edn. International Conference on Zn-Al Alloys. UNAM, March 1994; 195-200.
5. Aguilar MA, Pomar I, Hernández G, Fernández A, Piña C. A cytotoxicity test of the zinalco. In Torres G, Piña C, Zhu Y, eds. "Advances in Science", Technology and Applications of Zn-Al Alloys 3rd edn. International Conference on Zn-Al Alloys. March 1994; 201-3.
6. Aguilar MA, Espinosa S, Rodríguez L, Piña C. Biocompatibility *in vitro* tests of Zinalco. Mutat Res 1999; 446: 129-34.
7. Palma RB. Master Sc Thesis, Facultad de Ciencias, UNAM, Mexico 1999.
8. Pérez SN, Piña MC, Olivera A, et al. Estudio Preliminar de la Biocompatibilidad del Zinalco. Veterinaria México 1996; 27: 325-9.
9. Piña C, Torres K, Palma B, et al. Biocompatibility test to zinalco alloy. In: I Hernández, R Asomoza eds. Conference Proceedings 378 of Surfaces Vacuum and their Applications. New York: American Institute of Physics 1996; 354-8.
10. Piña C, Torres CK, Guzmán J. Histological study of connective tissue response to zinalco and SS-316L implants after 120 days. J Mater Sci Mater Med 1998; 9: 93-7.
11. Izquierdo MP, Piña MC, Pérez NS, Olivera AE, Luna del Villar J, Munguía N. Evaluación radiográfica de implantes zinalco en fémur de perros. Veterinaria México 1999; 30: 189-91.
12. Guía para el cuidado y uso de los animales de laboratorio. Ed. National Research Council, Ed. Mexicana. Academia Nacional de Medicina. Mexico 2002.
13. Flecknell PA. Laboratory animal anaesthesia. London: Academic Press 1987; 64-8, 103-5.
14. Pérez RA, Porra MJG, Merino DJC. Manual de analgesia y anestesia en el perro. México: McGraw Hill Interamericana 1999.
15. Kirk WR, Bonagura JD. Terapéutica veterinaria de pequeños animales 12th edn. Mexico: McGraw Hill Interamericana 1997; 1553 Guía 24-48, 75-8.
16. Especificaciones Técnicas para la producción, cuidado y uso de los animales de laboratorio. NOM-062-ZOO-1999.
17. Civjan S, Selting WJ, De Simon LB, Battistone GC, Grower MF. Characterization of osseous tissues by thermogravimetric and physical techniques. J Dent Res 1972; 51: 539-42.
18. Bigi G, Cojazzi S Panzavolta, et al. Structural analysis of turkey tendon collagen upon removal of the inorganic phase. J Inorg Biochem 1997; 68: 45-51.
19. Lozano L F. Estudio calorimétrico de colágena tipo I presente en hueso y su aplicación como técnica de análisis de restos óseos de interés arqueológico y paleontológico. Thesis, Facultad de Ciencias, UNAM, Mexico, 2002.
20. Turan B, Bayari S, Balcik C, Severcan F, Akkas N. A biomechanical and spectroscopic study of bone from rats with selenium deficiency and toxicity. Biometals 2000; 13: 113-21A.
21. Kaflak-Hachulsa, Kolodziejski W. Preliminary results on infrared microscopy of human bone. J Mol Struct 1999; 511- 512: 217-21.
22. Rey C, Collins B, Goehl T, Dickson R, Glimcher MJ. The carbonate environment in bone mineral: A resolution enhanced Fourier Transform Infrared Spectroscopy Study. Calcif Tissue Int 1989; 45: 157-64.
23. Rey C, Shimizu M, Collins B, Glimcher MJ. Resolution-Enhanced Fourier Transform Infrared Spectroscopy Study of the environment of phosphate ions in the early deposits of a solid phase of calcium phosphate in bone and enamel, their evolution with age. I: Investigations in the upsilon 4 PO4 domain. Calcif Tissue Int 1990; 46: 384.
24. Ito A, Ojima K, Naito H, Ichinose N, Tateishi T. Preparation, solubility, and cytocompatibility of zinc-releasing calcium phosphate ceramics. J Biomed Mater Res 2000; 50: 178-83.